

Anyon superconductivity and plateau transitions in doped fractional quantum anomalous Hall insulators

Pavel A. Nosov,* Zhaoyu Han,* and Eslam Khalaf

Department of Physics, Harvard University, Cambridge, MA 02138, USA

(Dated: June 4, 2025)

Recent experiments reported evidence of superconductivity and re-entrant integer quantum anomalous Hall (RIQAH) insulator upon doping the $\nu_e = 2/3$ fractional quantum anomalous Hall states (FQAH) in twisted MoTe₂, separated by narrow resistive regions. Anyons of a FQAH generally have a finite effective mass, and when described by anyon-flux composite fermions (CF), experience statistical magnetic fields with a commensurate filling. Here, we show that most of the experimental observations can be explained by invoking the effects of disorder on the Landau-Hofstadter bands of CFs. In particular, by making minimal assumptions about the anyon energetics and dispersion, we show that doping anyons drives plateau transitions of CFs into integer quantum Hall states, which physically corresponds to either to a superconductor or to a RIQAH phase. We develop a dictionary that allows us to infer the response in these phases and the critical regions from the knowledge of the response functions of the plateau transitions. In particular, this allows us to relate the superfluid stiffness of the superconductor to the polarizability of CFs. As a first step towards a quantitative understanding, we borrow results from the celebrated integer quantum Hall plateau transitions to make quantitative prediction for the critical behavior of the superfluid stiffness, longitudinal and Hall conductivity, and response to out-of-plane magnetic field, all of which agree reasonably well with the experimental observations. Our results provide strong support for anyon superconductivity being the mechanism for the observed superconductor in the vicinity of the $\nu_e = 2/3$ FQAH insulator.

Introduction—Superconductivity and the fractional quantum Hall (FQH) effects are two of the most iconic and well-studied quantum phases of matter. The realization of both phases in the same system is challenging since the large magnetic fields required to realize the FQH are generally incompatible with superconductivity. Moiré materials promise to overcome this difficulty due to their ability to host flat topological bands where FQH can be realized without an external magnetic field [1–17], dubbed fractional quantum anomalous Hall (FQAH) state. Recently, this promise was realized in the groundbreaking discoveries of FQAH first in twisted MoTe₂ (t-MoTe₂) [18–21] then in pentalayer rhombohedral graphene aligned to an hBN substrate [22].

Subsequent experiments have reported the remarkable discovery of superconductivity in these two systems. First, Ref. [23] reported the observation of superconductivity in moiréless rhombohedral graphene, which develops in the quarter metal phase where valley and spin are likely fully polarized and time-reversal is strongly broken. More recently, Ref. [24] reported the observation of superconductivity in a high-quality t-MoTe₂ sample. Remarkably, this phase emerges close to a FQAH state at filling fraction $\nu_e = 2/3$ of the moiré band, separated by a narrow resistive region on the doping axis. The vicinity of the $\nu_e = 2/3$ is also marked by several re-entrant integer quantum anomalous Hall (RIQAH) states realized by tuning either the doping ν_e or the vertical displacement field D . A sketch of the finite temperature experimental phase diagram, adapted from Ref. [24], as a function of ν_e and D is given in Fig. 1a.

The emergence of superconductivity upon doping an

FQAH suggests that it is possibly associated with the doped anyons. The idea of anyon superconductivity (SC) dates back to classic works of Laughlin [25–27], which suggested that a gas of itinerant anyons has a natural instability to SC. This arises from statistical interactions among anyons, which can be described by composite fermions (CF) coupled to a Chern-Simons (CS) gauge field. The CFs can be thought of as anyon-flux composites subject to a CS statistical flux density. Within a mean-field treatment, we can assume a uniform CS flux leading to Landau levels (LLs) of CFs. Due to the CS flux attachment relation, the density of the CFs is tied to the CS flux density, leading to a fixed LL filling. For certain types of anyons, this filling is an integer, thus can lead to an integer quantum Hall (IQH) state of CFs. Adding external magnetic flux to this state amounts to moving CFs across a LL gap, which cost a finite energy. This indicates the resulting phase is a superconductor (SC) [25–35].

Recently, Ref. [36] has revived this idea in the context of a doped FQAH and clarified important subtleties and distinctions compared to earlier construction. First, it was pointed out that the theory written in earlier works Ref. [25–28] cannot always emerge from microscopic theories of electrons. Second, it was emphasized that the phase realized upon doping a given FQAH depends on the species of anyons doped in the system and their detailed dispersion. An effective CF theory using a parton construction was derived to capture the physics [36].

A crucial distinction between the doped anyons of a FQAH realized in a lattice system compared to those of FQH in uniform field LLs is that the former can have a fi-

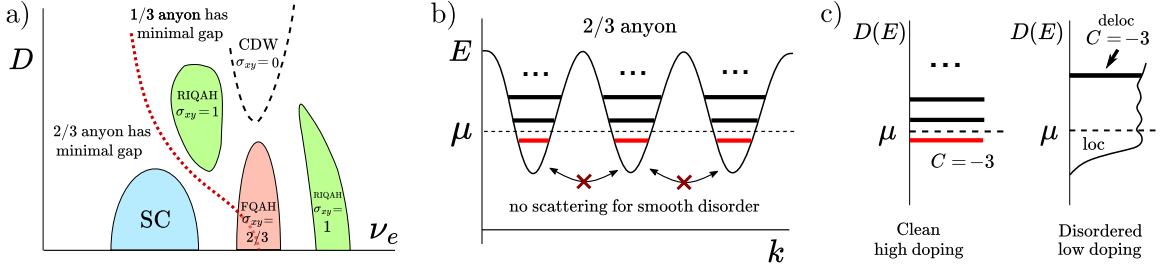


FIG. 1. a) Cartoon of the finite temperature phase diagram in the vicinity of the $\nu_e = 2/3$ FQAH state, as a function of doping ν_e and displacement field D (after [24]). The red dotted line separates regions where we assume that 2/3- and 1/3-anyons are energetically more favorable. b) 2/3-anyon dispersion with three minima in a Brillouin zone without disorder. Red solid lines denote filled LLs that appear due to statistical flux. Introduction of smooth potential disorder approximately preserves valley symmetry, but broadens levels within each valley. c) The density of states (with and without disorder) for the 2/3-anyons.

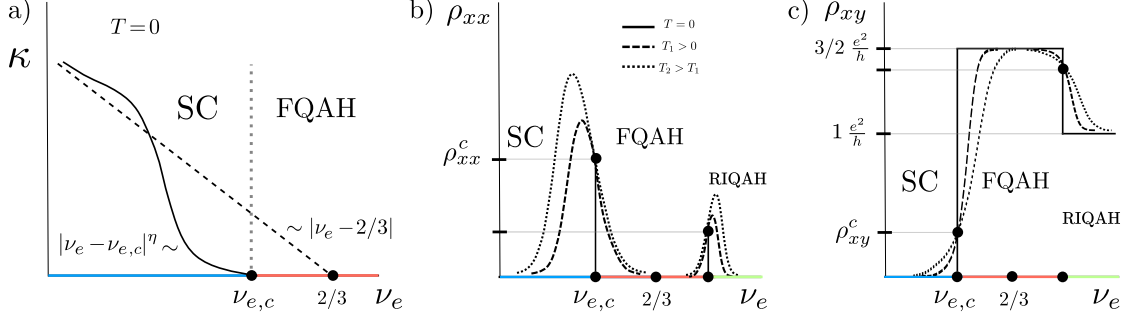


FIG. 2. a) Schematic behavior of the superfluid stiffness κ at $T = 0$ and $D = 0$ as a function of ν_e . b,c) Schematic behavior of the (b) longitudinal resistivity ρ_{xx} and (c) Hall resistivity ρ_{xy} as a function of doping, at several different temperatures.

nite dispersion due to the absence of continuous magnetic translation symmetry (MTS). This symmetry implies a uniform quantum geometry (Berry curvature, metric, and form factors) in momentum space and ensures that the dispersion of any charged excitation is perfectly flat. Thus, even though the single particle dispersion in the Chern bands of a FQAH is relatively flat, e.g. in t-MoTe₂ close to the magic angle, other charged quasiparticles, e.g. anyons, can acquire a dispersion due to non-uniform quantum geometry arising from the lack of continuous MTS. Importantly, while flat bands are needed for stabilizing FQAH phases, uniform quantum geometry is not required; recent work has identified a condition, called vortexability [37–46], that is sufficient to guarantee a Laughlin FQAH groundstate for short-range interactions, irrespective of the non-uniformity of quantum geometry. In fact, recent calculations suggest sizeable Berry curvature fluctuations in t-MoTe₂ flat bands [47, 48].

The mean-field picture of anyon superconductivity in terms of LLs of CFs subject to CS gauge field suggests that the transition between the FQAH and the SC can be understood as an integer quantum Hall (IQH) plateau transition of CFs. The analysis of such transition requires accounting for disorder-induced localization. In this paper, we show that localization effects yield a unified explanation for the emergence of superconductivity

and RIQAH states near the 2/3 FQAH and lead to quantitative predictions for conductance, superfluid stiffness, and response to out-of-plane magnetic field that are all in agreement with experiment [24].

Qualitative picture— Our results are summarized in Figs. 1 and 2. We consider doping a FQAH at fixed disorder strength. In terms of the CFs, doping induces an effective magnetic field, such that the only relevant energy scale at small doping is an effective cyclotron frequency, $\hbar\omega_c \propto |\delta\nu|$ where $\delta\nu \equiv \nu_e - 2/3$ is the doping concentration. To account for disorder, we introduce the scattering rate τ , which can be combined with ω_c to form a dimensionless measure of the disorder strength, $\omega_c\tau$. This parameter increases as a function of doping at a fixed τ , thus it is convenient to think of increasing doping as decreasing disorder strength.

There are two types of anyons with charge 2/3 and 1/3 which have self-statistical angles $-\pi/3$ and $2\pi/3$, respectively. Since the parent FQAH state can be viewed as already having one 2/3 anyon or two 1/3 anyons per unit cell, the doped anyons feel background effective magnetic field that triply folds the Brillouin zone (BZ), and a discrete MTS enforces the dispersion to be three-fold degenerate therein [36, 49] (illustrated in Fig. 1b). Upon doping 2/3 or 1/3 anyons, the additional statistical flux will reorganize the anyon bands into Landau-Hofstadter

sub-bands, and the rigid relation between charge and flux implies an effective filling fraction $\nu_{\text{eff}} = -3$ or $3/2$ of these *sub-bands* for the corresponding CFs, respectively.

At very small doping $\delta\nu \ll 1$, we can understand the Landau-Hofstadter bands as LLs forming in the 3-fold minima of the anyon dispersion, leading to 3-fold degenerate LLs. As doping is increased, this 3-fold degeneracy is lifted since the Hofstadter spectrum is generally non-degenerate (this will also be enhanced by disorder). The lifting of the degeneracy will depend on the details of the anyon dispersion, and should happen when $\hbar\omega_c \propto |\delta\nu|$ is of the same order as the energy barrier between the different minima. Therefore, we expect the degeneracy to be more robust if the potential minima are deep (Fig. 1b).

The effects of the disorder can be captured, at least on a qualitative level, by ignoring interactions between CFs and viewing the problem as that of LLs for single particles. We will discuss the validity of this assumption and possible caveats later. Borrowing results from IQH plateaus, we know that any amount of disorder will localize all states within a given LL except for a single extended state. For sufficiently strong disorder, such states will be pushed up in energy leading to a trivial state for CFs. Such state will precisely correspond to the parent FQAH. Doping charge effectively amounts to reducing disorder strength which results in the extended states going down in energy until they cross the chemical potential, leading to a plateau transition. The resulting state depends on the kind of doped anyon and on the number of extended states crossing the fermi energy.

A direct transition to a SC is realized if the doped charge goes in as a $2/3$ anyon *and* all three delocalized states are approximately degenerate and cross the Fermi energy simultaneously. This is the case if the minima of the $2/3$ anyon dispersion are relatively deep and if the disorder is sufficiently smooth such that it does not scatter between these minima (cf. Fig. 1b). This suggests that increasing the disorder or the effective mass of the anyon can lead to a splitting of this transition into 3 transitions. This may explain the shoulder feature observed in the resistive transition region in experiment [24]. On the other hand, a transition to a RIQAH is realized if the doped charge is a $1/3$ anyon and only one delocalized state is occupied. This suggests that $1/3$ anyons have a shallower dispersion and non-degenerate Hofstadter bands at the relevant doping. Physically, this implies a smaller characteristic energy scale for the RIQAH state compared to the SC, which is consistent to the experiment [24]. The resistive regions between the FQAH and either phase can be understood as IQH plateau transitions.

The phase diagram as a function of displacement field D can be attributed to changes in the anyon dispersion with D due to changes in the flat band quantum geometry. For instance, the observation that the SC (IQAH) phase boundary moves away from (towards) $2/3$ suggests the anyon effective mass (which controls the critical

$\omega_c\tau$) decreases (increases) with D for the $2/3(1/3)$ -anyon. Furthermore, the experiment suggests there is a phase boundary in the ν_e - D phase diagram where the cheapest charged excitation changes from $2/3$ - to $1/3$ -anyons. Energetically favored $2/3$ -anyons indicate a tendency of $1/3$ -anyons to pair as suggested by recent numerics [50, 51]. The prominence of this pairing on doping $2/3 + \delta\nu$ compared to $2/3 - \delta\nu$ is consistent with earlier results studying anyon energetics in Chern-Simons-Ginzburg-Landau theory of composite bosons [52].

Effective field theory— The starting point of our analysis is an effective Lagrangian describing anyons near a $\nu_e = 2/3$ FQAH state [36]:

$$\mathcal{L} = \mathcal{L}[\psi_{2/3}; a] + \mathcal{L}[\psi_{1/3}; b] + \mathcal{L}_{\text{CS}} + \mathcal{L}_{\text{dis}} + \mathcal{L}_{\text{int}} \quad (1)$$

$$\begin{aligned} \mathcal{L}_{\text{CS}} = & \frac{1}{2\pi} (b - a) dA + \frac{1}{4\pi} AdA + A_0 - b_0 \\ & - \frac{1}{4\pi} \begin{pmatrix} a & b \end{pmatrix} \begin{bmatrix} -2 & 1 \\ 1 & 1 \end{bmatrix} \begin{pmatrix} da \\ db \end{pmatrix} \end{aligned} \quad (2)$$

where $adb = \epsilon^{\mu\nu\eta} a_\mu \partial_\nu b_\eta$, a and b are emergent $U(1)$ gauge fields, and we have set the crystal unit cell area $\mathcal{A}_{\text{UC}} = 1$. $\psi_{2/3}$ and $\psi_{1/3}$ are two distinct CF fields, which represent, as we show below, the two types of anyons with charges $2/3$ and $1/3$. Finally, \mathcal{L}_{dis} encodes smooth disorder coupled to the density of electrons, and \mathcal{L}_{int} describes electron-electron interactions. A parton derivation of this action can be found in Ref. [36] and is reproduced in Supplemental Materials (SM) for completeness.

The equation of motion of a_0, b_0 yields the flux attachment conditions:

$$\begin{aligned} \frac{1}{2\pi} \begin{pmatrix} \nabla \times \mathbf{a} \\ \nabla \times \mathbf{b} \end{pmatrix} = & (\nu_{1/3} - 1) \begin{pmatrix} 1/3 \\ 2/3 \end{pmatrix} \\ & + \frac{B}{2\pi} \begin{pmatrix} 2/3 \\ 1/3 \end{pmatrix} + \nu_{2/3} \begin{pmatrix} -1/3 \\ 1/3 \end{pmatrix} \end{aligned} \quad (3)$$

where B is the external perpendicular magnetic field strength, $\nu_{a=2/3,1/3} \equiv \langle \psi_a^\dagger \psi_a \rangle$ are the average numbers of doped anyons per crystal unit cell (or simply the density, since we have set the unit cell area to 1). Therefore, the electron density (the source of A_0) can be evaluated as:

$$\nu_e = \frac{2}{3} \left(\frac{B}{2\pi} + 1 + \nu_{2/3} \right) + \frac{1}{3} \nu_{1/3} \quad (4)$$

which confirms that the system is a $2\pi\sigma_{xy} = \nu_e = 2/3$ state before doping. From Eq. S3 and S4, one can see that the $\psi_{2/3}, \psi_{1/3}$ have effective self-statistical angles $2\pi/3, -\pi/3$ and electric charges $2/3, 1/3$, respectively. Moreover they have mutual statistical angle $2\pi/3$. These features confirm that they describe the corresponding anyons. Depending on the details in the microscopic Hamiltonian, the two anyons may have different activation gaps such that the doped charge may enter the system as either type of the anyons. Below we will discuss the two cases separately.

Doping the 2/3-anyons— When the doped particles are 2/3-anyons, the corresponding CFs, $\psi_{2/3}$, are at effective filling fraction $\nu_{\text{eff}} = -3$ of their self statistical flux. Therefore, the most natural state is that $\psi_{2/3}$ form a IQH state with $C = -3$ described by $-\frac{3}{4\pi}ada$. The topological response theory describing the resulting state is:

$$\mathcal{L} = \frac{2}{2\pi}bdA + \frac{2}{4\pi}AdA - 2\Omega_g \quad (5)$$

where Ω_g is a gravitational CS term that originates from the framing anomaly of the CS fields [1, 4] [55]. The fact that a charge-2 current $J^\mu = \frac{2}{2\pi}\epsilon^{\mu\nu\eta}\partial_\nu b_\eta$ tends to screen the external magnetic field imply that this is a SC.

The phase stiffness of SC in 2D has the unit of energy and often limits the critical temperature T_c of the Berezinskii-Kosterlitz-Thouless transition out of the SC phase. In SM, we derive an expression for the stiffness in terms of the polarization tensor $\Pi^{\mu\nu} = \langle J^\mu J^\nu \rangle$ of $\psi_{2/3}$ by integrating out small fluctuations in the gauge field. We find that the inverse stiffness κ^{-1} is simply related to the polarizability $\chi_{2/3}$ of the $\psi_{2/3}$ state:

$$\kappa^{-1} = \frac{\chi_{2/3}}{(2\pi)^2} \equiv \lim_{q \rightarrow 0} \frac{\Pi^{00}}{q^2} \equiv \lim_{\omega \rightarrow 0} \lim_{q \rightarrow 0} \frac{\Pi^{ii}}{\omega^2}. \quad (6)$$

Deep in the SC phase, we expect $\omega_c\tau$ to be large (disorder effects are weak) since $\omega_c = \pi|\delta\nu|/m_{2/3}$. Previous work has evaluated χ in this case [2]. Building on this result we find

$$\kappa = \frac{\omega_c}{3\pi} \left(1 - \frac{\pi}{6\omega_c\tau} \right)^{-1}. \quad (7)$$

The negative sign of the correction in the denominator stems from the fact that the fermion polarizability in a lowest Landau level is reduced by weak disorder. For our problem, this gives rise to a weak enhancement of κ compared to the clean limit result. Note that this is very different from conventional BCS superconductors where weak disorder only suppresses coherence length and κ .

Transition region— As one approaches the transition region from the superconducting side, the density (and consequently the statistical flux density) decreases, indicating strong mixing between LLs within each valley due to potential scattering. In the limit $\omega_c\tau \ll 1$, the LLs significantly overlap, and all eigenstates become localized except for a discrete set of isolated extended (critical) states. These delocalized states originate near the centers of their respective Landau levels and gradually levitate relative to the Fermi level as the density continues to decrease. Thus, as long as the Fermi level stays within the mobility gap above the lowest delocalized level, the superconducting state is stable, and its stiffness can be extracted from the polarizability of the IQH state formed by $\psi_{2/3}$, which is given by $\chi \propto m_{2/3}\xi^2$ [3, 57], where ξ is the localization length. A derivation of this result from

Mott's argument is included in the SM. The dependence on ξ can be traced to the scaling of the dipole matrix elements $\langle m|\hat{x}_i|n\rangle \sim \xi$ in the current-current correlator Π^{ii} .

At some critical filling fraction $\nu_{e,c}$, the chemical potential coincides with the lowest delocalized state, signaling an IQH-insulator transition for $\psi_{2/3}$. Near this point, the localization length diverges as $\xi \sim 1/|\nu_e - \nu_{e,c}|^\nu$, where ν is the correlation length exponent characterizing the transition. As a result, the superfluid stiffness, which is inversely proportional to the polarizability Eq. (6), vanishes at this transition, and we find the following critical behavior for the zero-temperature stiffness:

$$\kappa(T=0) \propto |\nu_e - \nu_{e,c}|^\eta, \quad \eta = 2\nu. \quad (8)$$

On general grounds, we expect that $\nu \geq 1$ (and thus $\eta \geq 2$) due to the Harris criterion [59]. In particular, for the regular IQH-insulator transition, experiments find $\nu \approx 2.38 \pm 0.02$ [60, 61]. However, we emphasize that this value is merely suggestive as the actual critical exponent could be affected by the interplay between gauge fluctuations and disorder at the transition. Nevertheless, our simple analysis indicates that the stiffness should remain relatively low in the immediate vicinity of the transition, which could lead to much stronger temperature variations of the resistivity on the superconducting side of the plateau transition (see Fig. 2(b)). We note that this behavior was indeed observed in [24].

The critical filling $\nu_{e,c}$ can be roughly estimated from the well-known condition [5, 6] determining when the lowest critical state crosses the chemical potential (which in turn follows from the two-parameter scaling picture of the IQH-insulator transition). Applying this condition to our problem, we find

$$\frac{2}{3}\nu_{2/3,c} = \frac{-B_{\text{eff}}}{2\pi} \frac{1 + (\omega_c\tau)^2}{(\omega_c\tau)^2}, \quad (9)$$

where $\nu_{2/3,c}$ is the density of anyons, and $B_{\text{eff}} = -2\pi\nu_{2/3}/3$ is the effective magnetic field for $\psi_{2/3}$. This equation is applicable both for $\omega_c\tau \gg 1$ and $\omega_c\tau \ll 1$. From Eq. (9), we see that in the absence of external magnetic field, both B_{eff} and $\nu_{2/3,c}$ are proportional to the density of doped anyons. This yields an equation for $\omega_c\tau = \frac{\pi\tau|\delta\nu|}{m_{2/3}}$. Its solution is $\omega_c\tau \sim 1$ which gives a critical density $\delta\nu_c \sim \frac{m_{2/3}}{\tau}$. This condition can also be anticipated from the high-doping, weak-disorder side, even without invoking localization. It corresponds to the point at which the broadened Landau levels begin to overlap and the single-particle gap closes. Thus, the critical density increases with either increasing disorder strength or the anyon effective mass. This naturally explains why this transition will not be observed in very disordered samples or in FQH with continuous MTS where $m_{2/3}$ is infinite.

Using our dictionary to map the transition from FQAH to SC to an IQH plateau transition of CFs also enables us to express the conductivity tensor $\hat{\sigma}$ for electrons in terms of the conductivity tensor $\hat{\sigma}_{2/3}$ for $\psi_{2/3}$ as

$$2\pi\hat{\sigma} = 2\hat{E} - 4\hat{E} \cdot [2\pi\hat{\sigma}_{2/3} + 3\hat{E}]^{-1} \cdot \hat{E}, \quad (10)$$

where $(\hat{E})^{ij} = \epsilon^{ij}$ is the unit anti-symmetric tensor (see SM for the derivation). Under the assumption that $\psi_{2/3}$ is at the regular IQHI transition, the conductivity tensor then becomes $2\pi\hat{\sigma}_{2/3}^c = (3/2)(\hat{1} - \hat{E})$ [64] (the extra factor of 3 arises because of the valley degeneracy), and we find $2\pi\hat{\sigma}^c = \frac{4}{3}\hat{1} + \frac{2}{3}\hat{E}$. In this case, the longitudinal resistivity for electrons is $\rho_{xx}^c/2\pi = 3/5$ and the Hall resistivity is $|\rho_{xy}^c|/2\pi = 3/10$ at the SC-FQAH transition. This corresponds to a peak resistivity $\rho_{xx}^c \approx 15\text{k}\Omega$ in the transition region which is close to but slightly larger than the experimentally observed value [24]. We emphasize that actual value of $\sigma_{2/3,xx}^c$ may differ from the one obtained using the IQH plateau transition values due to effects of interactions and gauge fluctuations.

Finally, we note that a serious analysis of the critical point itself involves the interplay of disorder, electron-electron interactions and gauge fluctuations – a formidable task. While we do not attempt to explore this transition in full complexity here, it is useful to state the problem in the framework of Pruisken’s non-linear sigma model with a topological θ -term [5, 65, 66], which has been used before to study regular IQH transitions (see [67, 68] for review). For our problem, the effective Lagrangian necessarily includes a CS gauge field leading to:

$$\mathcal{L} = -\frac{3\pi}{4}\sigma_{2/3,xx}^{(0)} \text{Tr}[(\mathcal{D}_i Q)^2 - iz\partial_\tau Q - a_0 Q] + \frac{3\pi}{4}\sigma_{2/3,xy}^{(0)}\epsilon^{ij} \text{Tr}[Q\mathcal{D}_i Q\mathcal{D}_j Q] + \mathcal{L}_{\text{CS}} + \mathcal{L}_{\text{int}} \quad (11)$$

where $i, j=x, y$, $\mathcal{D}_\mu Q = \partial_\mu Q - i[\delta a_\mu, Q]$ which includes covariant coupling to the gauge field fluctuations δa_μ on top of the mean field state, the parameter z describes renormalization of the dynamical scaling exponent due to interactions [69], $N_r \rightarrow 0$ is the number of replicas. The constrained time bi-local matrix field $Q_{\tau,\tau'} \in U(12N_r)/U(6N_r) \times U(6N_r)$ encodes the density fluctuations of $\psi_{2/3}$ (i.e. heuristically $Q \sim \bar{\psi}_{2/3} \otimes \psi_{2/3}$), with the trace and multiplications involving both the matrix structure and convolutions for time arguments. Moreover, $\sigma_{2/3,xx}^{(0)}(\sigma_{2/3,xy}^{(0)})$ is the Drude conductivity per each valley, calculated within kinetic theory with the mean field effective flux experienced by $\psi_{2/3}$, possibly including effects of quenched flux disorder stemming from flux attachment constraint [70–74].

In addition to the presence of a CS gauge field and a non-standard coupling to the external field A (cf. Eq. (S2)), one important difference of Eq. (11) compared to the conventional (interacting) Pruisken’s sigma model

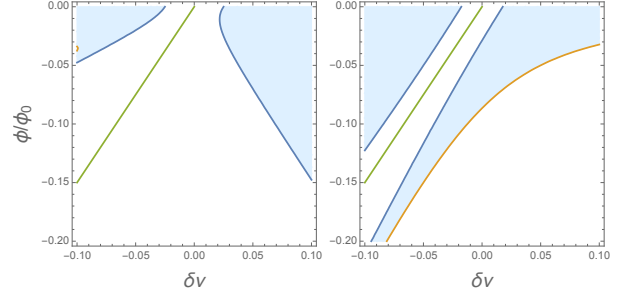


FIG. 3. The boundary of the phases of interest, which are shaded in the plot. ϕ/ϕ_0 is the flux per unit cell. (Left) the boundaries of anyon superconductor resulting from doped 2/3 anyons. (Right) the boundaries of RIQH state resulting from doped 1/3 anyons. The green line is defined by $\delta\nu = \frac{2}{3}\delta\nu_B$ which represents the center of FQAH state. The parameter used in these plots are $\frac{\pi\tau}{m} = 10$ for 1/3 anyons and $\frac{\pi\tau}{m} = 40$ for 2/3 anyons, so chosen such that the results agree reasonably with Ref. [24]. Note that, in principle, the masses of an anyon on the electron- or hole-doping sides may differ, but here we neglect this fact for simplicity.

[68, 75] is the existence of several approximately degenerate valleys, which allows for additional short-ranged interaction terms in \mathcal{L}_{int} , and thus potentially more complicated renormalization flow (in a single valley case, the short ranged interactions are known to be irrelevant at the transition [76–78]). Our previous considerations can be easily reproduced directly from Eq. (11) provided that we ignore interactions and integrate out gauge fluctuations perturbatively.

Doping the 1/3 anyon— We now briefly discuss the RIQAH along the same lines of our discussion of the FQAH to SC transition. When the doped particles are 1/3 anyons, they are at effective filling fraction $\nu_{\text{eff}} = 3/2$ of their self statistical flux. In the clean and small doping limit, we may expect a three-fold degenerate composite Fermi liquid (CFL) corresponding to the three potential minima [36]. However, we expect such state to be unstable to moderate disorder. Furthermore, we note that with disorder, the transition is expect to happen at finite doping where an effective LL description in each of the potential minima will break down if the dispersion is sufficiently shallow. Instead, we should consider the Landau-Hofstadter sub-bands, the lowest few of which are generally non-degenerate. Thus, we can effectively neglect the degeneracy between the valleys under the assumption that $m_{1/3}$ is large. Then, disorder will again localize most of the states in each sub-band except one state that carries the Hall response. Since the 1/3 anyon is at filling 3/2, at most one delocalized state can pass the chemical potential as the disorder strength is reduced, resulting in a $\frac{1}{4\pi}b\delta b$ response. The resulting effective response theory (after integrating out b which set $a = A$) is $\mathcal{L} = \frac{1}{4\pi}A\delta A + \Omega_g$ which describes an IQH state. An

analysis of the critical region similar to that for the $2/3$ anyons leads to $\rho_{1/3,xx}^c/2\pi = 1/5$ and $\rho_{1/3,xy}^c/2\pi = 7/5$. This corresponds to $\rho_{xx,1/3}^c \approx 5k\Omega$ which is very close to the value in experiment [24].

Effect of magnetic field— Upon applying an out-of-plane magnetic field, the density of CFs as well as the effective field strength felt by them will both change according to the flux attachment conditions Eq. S3 and Eq. S4. This can lead to phase transitions out of the phases of interest by moving the Fermi level of ψ across an extended state. To model this effect, we include the effect of external field in Eq. 9 to track the position of the extended states and the phase boundaries caused by the level crossing (See SM for details). The resulting phase boundaries of the anyon SC and RIQAH state caused by $\psi_{2/3}$ and $\psi_{1/3}$, respectively, are shown in Fig. 3. We find that the choice $\frac{\pi\tau}{m} = 10$ for $1/3$ anyons and $\frac{\pi\tau}{m} = 40$ for $2/3$ anyons, which is equivalent to choosing $m_{2/3} = m_{1/3}/4$ (see SM for details), approximately reproduces the experimentally observed phase boundaries [24]. This is consistent with our assumption of a shallower dispersion for the $1/3$ anyon.

Interestingly, we find that all the phase boundaries of the RIQAH state have a slope $\delta\nu/(\phi/\phi_0) \sim 0.6 < 1$ despite the state has $2\pi\sigma_{xy} = 1$. This violation of the Streda formula should not be surprising since the RIQAH is a compressible state. The dependence of the phase boundary on out-of-plane field seen in Fig. 3 can be understood by noting that the plateau transitions can be induced not only by varying the filling fractions but also by tuning $\omega_c\tau$ [5, 6]. For example, the phase boundaries of RIQAH state on the positive doping side in Fig. 3 are predominantly determined by the change of $\omega_c\tau$, resulting in a significant deviation from the Streda formula result. Indeed, this discrepancy has been observed in Ref. [24].

Conclusions— We have shown that by incorporating the effects of disorder-induced localization into an effective field theory describing the CFs of the $\nu_e = 2/3$ FQAH, we can explain the emergence of SC and RIQAH in its vicinity and the resistive regions between them. The main assumptions we made is that the doped charge at $\nu_e = 2/3 + \delta\nu$ enters the system as charge- $2/3$ anyons with deep well-developed 3-fold degenerate minima in dispersion whereas at $\nu_e = 2/3 - \delta\nu$, it enters as charge- $1/3$ anyons with shallow dispersion. Such assumptions can be examined by investigating the energetics of these excitations numerically which we leave for future works.

Our analysis enables us to interpret the resistive regions separating the FQAH and either the SC or RIQAH as plateau transitions of single or multiple flavors of CFs. Making the simplifying assumption that these transitions are in the same universality class as the IQH transition allows us to make concrete quantitative predictions about the critical behavior of the superfluid stiffness, longitudinal and Hall conductivity, and response to out-of-plane

magnetic field. Our predictions agree qualitatively and, in many cases, quantitatively with the experimental observations of Ref. [24]. Going beyond the non-interacting IQH plateau transition to include the effects of interactions and gauge fluctuations on these transitions is left to future works. We envision the possibility of analytically controlled treatments by taking the limit of large number of valleys [79] and/or large CS level.

We close by discussing few predictions for future experiments. Our results suggest that away from the clean limit, we generally expect small lifting of the CF LL degeneracy, which would split the transition between the FQAH to SC into 3 transitions with intervening RIQAH. Possible indication of such splitting can be seen in the shoulder feature in Ref. [24]. We expect this splitting to be more pronounced in more disordered samples (where disorder is not strong enough to completely destroy the SC), particularly for short-range disorder with large momentum scattering, or in parameter regimes (twist angle, displacement field, etc) where the $2/3$ anyon dispersion is shallow but it is still energetically favored compared to the $1/3$ anyon. We also expect the SC to have a large tunneling gap to single-particle excitations since the excitations of the normal state are not electron-like. An interesting question, which we leave to future works, is related to the nature of the normal state above the SC. Two natural possibilities are: a gas of preformed Cooper pairs or a gas of unpaired anyons. The former will lead to transport response that is similar to a BEC superconductor [80], whereas the latter may have distinct transport properties which remain largely unexplored [81].

Acknowledgements— We acknowledge Bert Halperin and Igor Burmistrov for fruitful discussions. We are grateful to Senthil Todadri and Darius Zhengyan Shi for informing us about an upcoming manuscript [82] whose content overlaps with this work and for coordinating submission. E. K. is supported by NSF MRSEC DMR-2308817 through the Center for Dynamics and Control of Materials. Z. H. is supported by a Simons Investigator award, the Simons Collaboration on Ultra-Quantum Matter, which is a grant from the Simons Foundation (651440).

* These authors contributed equally to this work.

- [1] Z. Liu and E. J. Bergholtz, Recent Developments in Fractional Chern Insulators (2022), arXiv:2208.08449 [cond-mat, physics:math-ph, physics:quant-ph].
- [2] S. A. Parameswaran, R. Roy, and S. L. Sondhi, C. R. Phys. **14**, 816 (2013).
- [3] E. J. Bergholtz and Z. Liu, Int. J. Mod. Phys. B **27**, 1330017 (2013), <https://doi.org/10.1142/S021797921330017X>.
- [4] T. Neupert, L. Santos, C. Chamon, and C. Mudry, Phys. Rev. Lett. **106**, 236804 (2011).

- [5] D. Sheng, Z.-C. Gu, K. Sun, and L. Sheng, Nat. Commun. **2**, 389 (2011).
- [6] N. Regnault and B. A. Bernevig, Phys. Rev. X **1**, 021014 (2011).
- [7] X.-L. Qi, Phys. Rev. Lett. **107**, 126803 (2011).
- [8] S. A. Parameswaran, R. Roy, and S. L. Sondhi, Phys. Rev. B **85**, 241308 (2012).
- [9] Y.-L. Wu, N. Regnault, and B. A. Bernevig, Phys. Rev. Lett. **110**, 106802 (2013).
- [10] S. Kourtis, T. Neupert, C. Chamon, and C. Mudry, Physical Review Letters **112**, 126806 (2014), arXiv:1310.6371 [cond-mat].
- [11] G. Tarnopolsky, A. J. Kruchkov, and A. Vishwanath, Phys. Rev. Lett. **122**, 106405 (2019).
- [12] P. J. Ledwith, G. Tarnopolsky, E. Khalaf, and A. Vishwanath, Phys. Rev. Research **2**, 023237 (2020).
- [13] J. Wang, Y. Zheng, A. J. Millis, and J. Cano, Phys. Rev. Research **3**, 023155 (2021).
- [14] B. Mera and T. Ozawa, Phys. Rev. B **104**, 115160 (2021).
- [15] B. Mera and T. Ozawa, Phys. Rev. B **104**, 045104 (2021).
- [16] P. J. Ledwith, A. Vishwanath, and E. Khalaf, Phys. Rev. Lett. **128**, 176404 (2022).
- [17] P. J. Ledwith, A. Vishwanath, and D. E. Parker, (2022), arXiv: 2209.15023.
- [18] J. Cai, E. Anderson, C. Wang, X. Zhang, X. Liu, W. Holtzmann, Y. Zhang, F. Fan, T. Taniguchi, K. Watanabe, Y. Ran, T. Cao, L. Fu, D. Xiao, W. Yao, and X. Xu, Nature **622**, 63 (2023).
- [19] Y. Zeng, Z. Xia, K. Kang, J. Zhu, P. Knüppel, C. Vaswani, K. Watanabe, T. Taniguchi, K. F. Mak, and J. Shan, Nature **622**, 69 (2023).
- [20] H. Park, J. Cai, E. Anderson, Y. Zhang, J. Zhu, X. Liu, C. Wang, W. Holtzmann, C. Hu, Z. Liu, T. Taniguchi, K. Watanabe, J.-H. Chu, T. Cao, L. Fu, W. Yao, C.-Z. Chang, D. Cobden, D. Xiao, and X. Xu, Nature **622**, 74 (2023).
- [21] F. Xu, Z. Sun, T. Jia, C. Liu, C. Xu, C. Li, Y. Gu, K. Watanabe, T. Taniguchi, B. Tong, J. Jia, Z. Shi, S. Jiang, Y. Zhang, X. Liu, and T. Li, Phys. Rev. X **13**, 031037 (2023).
- [22] Z. Lu, T. Han, Y. Yao, A. P. Reddy, J. Yang, J. Seo, K. Watanabe, T. Taniguchi, L. Fu, and L. Ju, Nature **626**, 759 (2024).
- [23] T. Han, Z. Lu, Z. Hadjri, L. Shi, Z. Wu, W. Xu, Y. Yao, A. A. Cotten, O. S. Sedeh, H. Weldeyesus, *et al.*, Nature, **1** (2025).
- [24] F. Xu, Z. Sun, J. Li, C. Zheng, C. Xu, J. Gao, T. Jia, K. Watanabe, T. Taniguchi, B. Tong, *et al.*, arXiv preprint arXiv:2504.06972 (2025).
- [25] R. B. Laughlin, Phys. Rev. Lett. **60**, 2677 (1988).
- [26] R. B. Laughlin, Science **242**, 525 (1988), <https://www.science.org/doi/pdf/10.1126/science.242.4878.525>.
- [27] A. Fetter, C. Hanna, and R. Laughlin, Physical Review B **39**, 9679 (1989).
- [28] Y.-H. Chen, F. Wilczek, E. Witten, and B. I. Halperin, International Journal of Modern Physics B **3**, 1001 (1989).
- [29] D.-H. Lee and M. P. A. Fisher, Phys. Rev. Lett. **63**, 903 (1989).
- [30] S. Divic, V. Crépel, T. Soejima, X.-Y. Song, A. Millis, M. P. Zaletel, and A. Vishwanath, arXiv preprint arXiv:2410.18175 (2024).
- [31] X. G. Wen, F. Wilczek, and A. Zee, Phys. Rev. B **39**, 11413 (1989).
- [32] Y. Hosotani and S. Chakravarty, Phys. Rev. B **42**, 342 (1990).
- [33] X. G. Wen and A. Zee, Phys. Rev. B **41**, 240 (1990).
- [34] D.-H. Lee, International Journal of Modern Physics B **05**, 1695 (1991), <https://doi.org/10.1142/S0217979291001607>.
- [35] Y. Kitazawa and H. Murayama, Phys. Rev. B **41**, 11101 (1990).
- [36] Z. D. Shi and T. Senthil, arXiv preprint arXiv:2409.20567 (2024).
- [37] R. Roy, Phys. Rev. B **90**, 165139 (2014).
- [38] T. S. Jackson, G. Möller, and R. Roy, Nat Commun **6**, 8629 (2015).
- [39] M. Claassen, C. H. Lee, R. Thomale, X.-L. Qi, and T. P. Devereaux, Phys. Rev. Lett. **114**, 236802 (2015).
- [40] C. H. Lee, M. Claassen, and R. Thomale, Phys. Rev. B **96**, 165150 (2017).
- [41] P. J. Ledwith, G. Tarnopolsky, E. Khalaf, and A. Vishwanath, Phys. Rev. Research **2**, 023237 (2020).
- [42] T. Ozawa and B. Mera, Phys. Rev. B **104**, 045103 (2021).
- [43] B. Mera and T. Ozawa, Phys. Rev. B **104**, 045104 (2021).
- [44] B. Mera and T. Ozawa, Phys. Rev. B **104**, 115160 (2021).
- [45] J. Wang, J. Cano, A. J. Millis, Z. Liu, and B. Yang, Phys. Rev. Lett. **127**, 246403 (2021).
- [46] P. J. Ledwith, A. Vishwanath, and D. E. Parker, Phys. Rev. B **108**, 205144 (2023).
- [47] J. Dong, J. Wang, P. J. Ledwith, A. Vishwanath, and D. E. Parker, Phys. Rev. Lett. **131**, 136502 (2023).
- [48] J. Shi, N. Morales-Durán, E. Khalaf, and A. H. MacDonald, Phys. Rev. B **110**, 035130 (2024).
- [49] S. Musser, M. Cheng, and T. Senthil, arXiv preprint arXiv:2408.03984 (2024).
- [50] Q. Xu, G. Ji, Y. Wang, H. Q. Trung, and B. Yang, arXiv preprint arXiv:2505.20257 (2025).
- [51] M. Gattu and J. K. Jain, arXiv preprint arXiv:2505.22782 (2025).
- [52] R. Tafelmayer, Nuclear Physics B **396**, 386 (1993).
- [4] A. Gromov, G. Y. Cho, Y. You, A. G. Abanov, and E. Fradkin, Phys. Rev. Lett. **114**, 016805 (2015).
- [1] A. G. Abanov and A. Gromov, Phys. Rev. B **90**, 014435 (2014).
- [55] The coefficient (-2) is the chiral central charge c_- of the system [8].
- [2] I. Burmistrov, Journal of Experimental and Theoretical Physics **95**, 132 (2002).
- [57] O. Viehweger and K. B. Efetov, Phys. Rev. B **44**, 1168 (1991).
- [3] M. V. Feigel'man, D. A. Ivanov, and E. Cuevas, New Journal of Physics **20**, 053045 (2018).
- [59] A. B. Harris, Journal of Physics C: Solid State Physics **7**, 1671 (1974).
- [60] W. Li, G. A. Csáthy, D. C. Tsui, L. N. Pfeiffer, and K. W. West, Phys. Rev. Lett. **94**, 206807 (2005).
- [61] W. Li, C. L. Vicente, J. S. Xia, W. Pan, D. C. Tsui, L. N. Pfeiffer, and K. W. West, Phys. Rev. Lett. **102**, 216801 (2009).
- [6] R. B. Laughlin, Phys. Rev. Lett. **52**, 2304 (1984).
- [5] D. Khmel'nitskii, JETP Lett. **38** (9), 552 (1983).
- [64] P. Kumar, Y. B. Kim, and S. Raghu, Phys. Rev. B **100**, 235124 (2019).
- [65] H. Levine, S. B. Libby, and A. M. M. Pruiskien, Phys. Rev. Lett. **51**, 1915 (1983).
- [66] R. B. Laughlin, Phys. Rev. Lett. **50**, 1395 (1983).
- [67] F. Evers and A. D. Mirlin, Rev. Mod. Phys. **80**, 1355 (2008).

- [68] I. S. Burmistrov, Journal of Experimental and Theoretical Physics **129**, 669 (2019).
- [69] D. Belitz and T. R. Kirkpatrick, Rev. Mod. Phys. **66**, 261 (1994).
- [70] S. A. Kivelson, D.-H. Lee, Y. Krotov, and J. Gan, Phys. Rev. B **55**, 15552 (1997).
- [71] A. G. Aronov, A. D. Mirlin, and P. Wölfle, Phys. Rev. B **49**, 16609 (1994).
- [72] C. Wang, N. R. Cooper, B. I. Halperin, and A. Stern, Phys. Rev. X **7**, 031029 (2017).
- [73] P. Kumar, S. Raghu, and M. Mulligan, Phys. Rev. B **99**, 235114 (2019).
- [74] P. Kumar, P. A. Nosov, and S. Raghu, Phys. Rev. Res. **4**, 033146 (2022).
- [75] A. M. M. Pruisken and M. A. Baranov, Europhysics Letters **31**, 543 (1995).
- [76] D.-H. Lee and Z. Wang, Phys. Rev. Lett. **76**, 4014 (1996).
- [77] Z. Wang, M. P. A. Fisher, S. M. Girvin, and J. T. Chalker, Phys. Rev. B **61**, 8326 (2000).
- [78] I. Burmistrov, S. Bera, F. Evers, I. Gornyi, and A. Mirlin, Annals of Physics **326**, 1457 (2011).
- [79] A. Punnoose and A. M. Finkel'stein, Science **310**, 289 (2005), <https://www.science.org/doi/pdf/10.1126/science.1115660>.
- [80] Q. Chen, J. Stajic, S. Tan, and K. Levin, Physics Reports **412**, 1 (2005).
- [81] B. I. Halperin, Phys. Rev. B **45**, 5504 (1992).
- [82] Z. D. Shi and T. Senthil, to appear.
- [8] N. Seiberg, T. Senthil, C. Wang, and E. Witten, Annals of Physics **374**, 395 (2016).

ANYON SUPERCONDUCTIVITY AND PLATEAU TRANSITIONS IN DOPED FRACTIONAL QUANTUM ANOMALOUS HALL INSULATORS: SUPPLEMENTAL MATERIALS

DETAILS OF THE MODEL SETUP

Throughout this paper, we adopt the following convention: Greek letters (μ, ν, \dots) are used for spacetime indices, and Latin letters (i, j, \dots) are used only for the spatial indices; the sign convention is such that $a^\mu = (t, \mathbf{a}_i)$, $\partial^\mu = (\partial_t, -\nabla_i)$ and the metric $g_{\mu\nu} = \text{diag}(1, -1, -1)$ for flat spacetime. Bold symbols are reserved for the spatial components of physical vectors, while arrow symbols are used for abstract vectors. Repeated indices in equations indicate implicit summations over them. We absorb a factor of electron charge $|e|$ in the definition of gauge fields, and adopt units such that $\hbar = c = 1$.

In this work, we work with the following effective Lagrangian describing anyons near a $\nu = 2/3$ FQAH state:

$$\mathcal{L} = \mathcal{L}[\psi_{2/3}; a] + \mathcal{L}[\psi_{1/3}; b] + \mathcal{L}_{\text{CS}} + \mathcal{L}_{\text{dis}} \quad (\text{S1})$$

$$\begin{aligned} \mathcal{L}_{\text{CS}} = & \frac{1}{2\pi} (b - a) dA + \frac{1}{4\pi} A dA + \frac{1}{\mathcal{A}_{\text{UC}}} (A_0 - b_0) \\ & - \frac{1}{4\pi} \begin{pmatrix} a & b \end{pmatrix} \begin{bmatrix} -2 & 1 \\ 1 & 1 \end{bmatrix} \begin{pmatrix} a \\ b \end{pmatrix} \end{aligned} \quad (\text{S2})$$

where we have adopted a short-handed notation for exterior derivatives, e.g. $adb = \epsilon^{\mu\nu\eta} a_\mu \partial_\nu b_\eta$, a and b are emergent $U(1)$ gauge fields, and \mathcal{A}_{UC} is the area of a crystal unit cell. $\psi_{2/3}$ and $\psi_{1/3}$ are two distinct fermionic matter fields, which represent, as we will see below, the two types of anyons with charges $2/3$ and $1/3$, and “;” symbols separate them and the emergent gauge fields they couple to. A parton derivation of this action can be found in Sec. . In the main text, we set $\mathcal{A}_{\text{UC}} = 1$ for simplicity, but here we will keep it to make the dependence explicit. We also keep the distinction between densities ρ and filling ν .

The equation of motion of a_0, b_0 yields the flux attachment conditions:

$$\frac{1}{2\pi} \left(\frac{\nabla \times \mathbf{a}}{\nabla \times \mathbf{b}} \right) = \frac{B}{2\pi} \left(\frac{2/3}{1/3} \right) + \left(\rho_{1/3} - \frac{1}{\mathcal{A}_{\text{UC}}} \right) \left(\frac{1/3}{2/3} \right) + \rho_{2/3} \left(\frac{-1/3}{1/3} \right) \quad (\text{S3})$$

where B is the external perpendicular magnetic field strength, $\rho \equiv \psi^\dagger \psi$ are the densities of the anyons. Therefore, the electron density (the source of A_0) can be evaluated as:

$$\rho_e = \frac{1}{\mathcal{A}_{\text{UC}}} + \frac{\nabla \times (\mathbf{b} - \mathbf{a}) + B}{2\pi} = \frac{2}{3} \left(\frac{B}{2\pi} + \frac{1}{\mathcal{A}_{\text{UC}}} + \rho_{2/3} \right) + \frac{1}{3} \rho_{1/3} \quad (\text{S4})$$

which confirms that the system is a $2\pi\sigma_{xy} = \nu = 2/3$ state.

We assume the disorder field couples to the density of electrons. Therefore, the effective theory is

$$\mathcal{L}_{\text{dis}} = V_{\text{dis}}(\mathbf{r}) \left[\frac{2}{3} \rho_{2/3}(\mathbf{r}) + \frac{1}{3} \rho_{1/3}(\mathbf{r}) \right] \quad (\text{S5})$$

where we introduced a random Gaussian quenched potential $V_{\text{dis}}(\mathbf{r})$ with the following properties

$$\overline{V_{\text{dis}}(\mathbf{r})} = 0, \quad \overline{V_{\text{dis}}(\mathbf{r})V_{\text{dis}}(\mathbf{r}')} = W(\mathbf{r} - \mathbf{r}'). \quad (\text{S6})$$

Here we allow $W(\mathbf{r})$ to have a finite correlation length d . In the limiting case of white-noise disorder, $W(\mathbf{r})$ reduces to a delta-function $W(\mathbf{r}) = \delta(\mathbf{r})/2\pi\nu\tau$. Here $\mathcal{D}_0 = m/2\pi$ is the density of states, and τ is the mean-free time between elastic collisions. If the potential was just given by a sum of uniformly-distributed delta peaks $V_{\text{dis}}(\mathbf{r}) = u \sum_i \delta(\mathbf{r} - \mathbf{r}_i)$, then the scattering rate would be given by $\tau^{-1} = mn_{\text{imp}}u^2$ (here n_{imp} is the density of impurities). Note that it is independent of the anyon density because the density of states for a parabolic dispersion in 2D is a constant.

From Eq. S3 and S4, one can see that the $\psi_{2/3}, \psi_{1/3}$ have effective self-statistical angle $\theta = 2\pi/3, -\pi/3$ and electric charge $Q = 2/3, 1/3$, respectively. Moreover they have mutual statistical angle $\theta = -2\pi/3$. These features confirm that they describe the corresponding anyons.

We will consider the states that can arise with light doping and small perpendicular fields. Under this setup, the emergent gauge fields a, b have approximate flux density per unit cell $-1/3, -2/3$, which suggests that the anyon bands should be considered in a magnetic unit cell that triples the crystal unit cell. Within the magnetic unit cell, all the anyon bands have dispersions with three-fold degeneracy ensured by the magnetic translation symmetry.

Depending on the details in the microscopic Hamiltonian, the two anyons may have different activation gaps such that the doped charge may enter the system as either $1/3$ or $2/3$ anyons. In the following sections, we will discuss these two cases separately.

Doping the $2/3$ -anyons: anyon superconductor

When doped particles are $2/3$ anyons, they are at effective filling fraction $\nu_{\text{eff}} = -3$ of their self statistical flux. Therefore, the most natural state is that $\psi_{2/3}$ form a IQH state with $C = -3$ described by $-\frac{3}{4\pi}ada$. The effective response theory describing the resulting state is:

$$\begin{aligned} \mathcal{L} &= \frac{1}{2\pi} (b - a) dA + \frac{1}{4\pi} AdA - \frac{1}{4\pi} (a + b) d(a + b) - 3\Omega_g \\ &= \frac{2}{2\pi} bdA + \frac{2}{4\pi} AdA - 2\Omega_g \end{aligned} \quad (\text{S7})$$

where in the second equality we have defined $\alpha \equiv a + b$ and integrated it out, Ω_g is a gravitational CS term that originates from the framing anomaly of the CS fields [1, 4]. (After integrating out all the dynamical gauge fields, its coefficient is the chiral central charge of the edge of the system [8], so we will explicitly keep track of this term, even though we are not going into its details.) This describes a charge-2 superconductor with current field $J = \frac{2}{2\pi} \star db$ where \star is the Hodge dual operation and chiral central charge $c_- = -2$.

Doping the $1/3$ -anyons: re-entrant integer quantum Hall state

When the doped particles are $1/3$ anyons, they are at effective filling fraction $\nu_{\text{eff}} = 3/2$ of their self statistical flux. In the clean and dilute limit, there is no simple gapped state to form corresponding to this filling fraction, especially given the triple degeneracy of the effective LLs at the three valleys of the magnetic Brillouin zone (BZ). However, with finite doping concentration, we should really be thinking about the Landau-Hofstadter subbands formed in this system, the lowest few of which can be quickly non-degenerate as long as the dispersion of the anyon is shallow. Effectively, we may neglect the degeneracy between valleys under the assumption that $\psi_{1/3}$ anyons' effective mass is large. Then, disorder will again localize most of the states in each band except one state that carries the Hall response, and the levitation of the extended states may separate them such that only one of them is occupied by $\psi_{1/3}$ at the filling fraction, resulting in a $\frac{1}{4\pi}bdb$ response. The resulting effective response theory of this scenario is

$$\begin{aligned} \mathcal{L} &= \frac{1}{2\pi} (b - a) dA + \frac{1}{4\pi} AdA + \frac{2}{4\pi} ada - \frac{1}{2\pi} adb + \Omega_g \\ &= \frac{1}{4\pi} AdA + \Omega_g \end{aligned} \quad (\text{S8})$$

where in the second step we integrated out b which yields $a = A$. This describe an IQH state.

PARTON DERIVATION OF THE EFFECTIVE THEORY

Here we briefly derive the effective theory, Eq. S1 used in the main text, with a parton decomposition $\psi_e = f_1 f_2 f_3$ of electrons. This derivation largely coincides with that used in Ref. [9], up to some convention difference. We choose charge assignment:

$$\mathcal{L} = \mathcal{L}[f_1; a] + \mathcal{L}[f_2; -b] + \mathcal{L}[f_3; A - a + b] \quad (\text{S9})$$

for the emergent $U(1)$ gauge fields which glue the partons together. For the undoped case $\nu = 2/3$, we assume the flux assignment:

$$\frac{\langle \nabla \times \mathbf{a} \rangle}{2\pi} = -\frac{1}{3} \frac{1}{\mathcal{A}_{\text{UC}}}, \quad \frac{\langle \nabla \times \mathbf{b} \rangle}{2\pi} = -\frac{2}{3} \frac{1}{\mathcal{A}_{\text{UC}}} \quad (\text{S10})$$

such that the each parton band of a crystal BZ is reorganized into three Hofstadter sub-bands of a magnetic BZ, and two of them are filled for each type of parton according to the filling fraction. To obtain the correct response function, we assume that the f_1, f_3 partons form $C_1 = C_3 = 1$ Chern insulators, and f_2 form $C_2 = -2$ Chern insulator. This means that, in terms of the Diophantine equation of the Hofstadter problem

$$\frac{n}{n_0} = \frac{\phi}{\phi_0} C + S \quad (\text{S11})$$

we assumed $S_1 = S_3 = 1$ and $S_2 = 2$. Since the effective response theory of such a Chern insulator is given by $\frac{C}{4\pi} \text{Ad}A + A_0 S + C \Omega_g$, the resulting effective theory is

$$\begin{aligned} \mathcal{L} &= \frac{1}{4\pi} a da + a_0 \frac{1}{\mathcal{A}_{\text{UC}}} + \Omega_g \\ &\quad - \frac{2}{4\pi} b db - 2b_0 \frac{1}{\mathcal{A}_{\text{UC}}} - 2\Omega_g \\ &\quad + \frac{1}{4\pi} (A - a + b) d(A - a + b) + (A_0 - a_0 + b_0) \frac{1}{\mathcal{A}_{\text{UC}}} + \Omega_g \\ &= \frac{2}{4\pi} a da - \frac{1}{4\pi} b db - \frac{1}{2\pi} a db + \frac{1}{2\pi} (b - a) dA + \frac{1}{4\pi} \text{Ad}A + \frac{1}{\mathcal{A}_{\text{UC}}} (A_0 - b_0) \end{aligned} \quad (\text{S12})$$

Now let's consider the doped cases with excitations. These will be the parton excitations that deviate from the Chern insulator state assumed above. More specifically we will assume that the f_3 partons are much more gapped than f_1 and f_2 , and re-name the particle excitations of f_1 with $\psi_{2/3}$ and the hole excitations of f_2 with $\psi_{1/3}$. Adding the actions of these fields to the theory above reproduces the anyon theory Eq. S1.

THE RESPONSE THEORY

General discussion

The physical response of the electrons can be obtained at mean-field level in terms of the response of the anyons fields, ψ , as follows.

We will assume weak fluctuations of the emergent gauge fields, such that the response of the ψ fields to the gauge fields can be effectively captured by the corresponding polarization tensor $\Pi^{\mu\nu} = \langle J^\mu J^\nu \rangle$ in a way that the effective action is quadratic in the fluctuating part of the gauge fields $\delta a, \delta b$. In the two cases of $2/3$ or $1/3$ anyons doped into the system, the effective response theory respectively reads:

$$\mathcal{L} = \frac{1}{2} \delta a_\mu \Pi_{2/3}^{\mu\nu} \delta a_\nu + \frac{3}{4\pi} \delta a d \delta a - \frac{2}{2\pi} \delta a d A + \frac{2}{4\pi} \text{Ad}A \quad (\text{S13})$$

$$\mathcal{L} \sim \frac{1}{2} \delta b_\mu \Pi_{1/3}^{\mu\nu} \delta b_\nu - \frac{3}{2} \frac{1}{4\pi} \delta b d \delta b + \frac{1}{2} \frac{1}{2\pi} \delta b d A + \frac{1}{2} \frac{1}{4\pi} \text{Ad}A \quad (\text{S14})$$

where we used the \sim symbol in the second case since the quantization of the CS terms has been relaxed since we are only interested in the response functions here. For simplicity, we then take the temporal gauge for all the gauge

fields ($a_0 = b_0 = A_0 = 0$). Then further integrating out δa or δb yields the following expressions for the physical polarization tensor of electrons and thus the conductivity in the two cases, respectively:

$$\begin{aligned} 2\pi\sigma_e^{ij}(\mathbf{q}, \omega) &= 2\pi\Pi_e^{ij}(\mathbf{q}, \omega)/(\mathrm{i}\omega) = 2E - 4\mathrm{i}\omega E \cdot [2\pi\Pi_{2/3} + 3\mathrm{i}\omega E]^{-1} \cdot E \\ &= 2E - 4E \cdot [2\pi\sigma_{2/3} + 3E]^{-1} \cdot E \end{aligned} \quad (\text{S15})$$

$$2\pi\sigma_e^{ij}(\mathbf{q}, \omega) = 2\pi\Pi_e^{ij}(\mathbf{q}, \omega)/(\mathrm{i}\omega) = \frac{1}{2}E - \frac{1}{4}E \cdot [2\pi\sigma_{1/3} - \frac{3}{2}E]^{-1} \cdot E \quad (\text{S16})$$

where

$$E \equiv \begin{bmatrix} 0 & 1 \\ -1 & 0 \end{bmatrix} \quad (\text{S17})$$

For example, at the critical point of the two possible plateau transitions at zero temperature discussed in the main text, we expect

$$2\pi\sigma_{2/3} = 3/2(I - E) \quad (\text{S18})$$

$$2\pi\sigma_{1/3} = 1/2(I + E) \quad (\text{S19})$$

where I is the identity. This means that the electron conductivity in the two cases is, respectively,

$$2\pi\sigma_e = \frac{4}{3}I + \frac{2}{3}E \quad (\text{S20})$$

$$2\pi\sigma_e = \frac{1}{10}I + \frac{7}{10}E \quad (\text{S21})$$

which means the resistivity

$$\rho_e/(2\pi) = \frac{3}{5}I - \frac{3}{10}E \quad (\text{S22})$$

$$\rho_e/(2\pi) = \frac{1}{5}I - \frac{7}{5}E \quad (\text{S23})$$

Special care for the superconducting case

For the superconducting state, the compactness of the gauge fields is essential for obtaining the correct response theory. Technically, δa cannot be integrated out in such a phase but requires a more careful treatment as follows.

Generically, the polarization tensor (generated by $\psi_{2/3}$) can be decomposed to:

$$\Pi_{\mu\nu}(q) = \sum_i \varpi^{(i)}(q) T_{\mu\nu}^{(i)}(q) \quad (\text{S24})$$

$$T_{\mu\nu}^{(i=0,1,2)}(q) = v_\mu^{(i)} v_\nu^{(i)}, \quad v_\mu^{(i)} = \frac{1}{2\pi} \epsilon_{i\mu\nu} q_\nu \quad (\text{S25})$$

$$T_{\mu\nu}^{(i=3)}(q) = \frac{1}{2\pi} \mathrm{i} \epsilon_{\mu\nu\eta} q_\eta \quad (\text{S26})$$

Or more explicitly

$$\Pi_{\mu\nu}(\mathbf{q}, \omega) = \frac{\varpi^{(0)}}{(2\pi)^2} \begin{bmatrix} 0 & 0 & 0 \\ 0 & q_y^2 & -q_x q_y \\ 0 & -q_x q_y & q_x^2 \end{bmatrix} + \frac{\varpi^{(1)}}{(2\pi)^2} \begin{bmatrix} q_y^2 & 0 & -\omega q_y \\ 0 & 0 & 0 \\ -\omega q_y & 0 & \omega^2 \end{bmatrix} + \frac{\varpi^{(2)}}{(2\pi)^2} \begin{bmatrix} q_x^2 & -\omega q_x & 0 \\ -\omega q_x & \omega^2 & 0 \\ 0 & 0 & 0 \end{bmatrix} + \frac{\mathrm{i}\varpi^{(3)}}{2\pi} \begin{bmatrix} 0 & q_y & -q_x \\ -q_y & 0 & \omega \\ q_x & -\omega & 0 \end{bmatrix} \quad (\text{S27})$$

In 2 + 1d, any compact $U(1)$ dynamical gauge field, e.g. a , admits a dual representation:

$$J^\mu = \frac{1}{2\pi} \epsilon^{\mu\nu\eta} \partial_\nu a_\eta \quad (\text{S28})$$

subject to the continuity constraint $\partial_\mu J^\mu = 0$ which can be enforced by $U(1)$ Lagrangian multiplier θ . This allows us to rewrite the Lagrangian at three-momentum q into the form:

$$L(q) = \frac{1}{2} \sum_{\mu=0,1,2} \varpi^{(\mu)} J_\mu J^\mu + \frac{2\pi[3 + \varpi^{(3)}]}{2} \epsilon^{\mu\nu\eta} J_\mu J_\nu \frac{1}{iq_\eta} + (iq_\mu \theta - 2A_\mu) J^\mu \quad (\text{S29})$$

Then, integrating out J , we obtain the final effective action

$$L(q) = \frac{\kappa^{\mu\nu}}{2} (iq\theta - 2A)_\mu (iq\theta - 2A)_\nu \quad (\text{S30})$$

where κ is the inverse of the kernel of J .

For the case where $\varpi^{(3)} = -3$ cancels the native CS term, we find the action is exactly the effective action of a charge- $2e$ superconductor. From its expression we can extract the dictionary between the compressibility κ^t and stiffness κ (assuming rotational invariance) for the electrons and the polarization tensor of the $\psi_{2/3}$ anyons:

$$1/\kappa^0 = \varpi^{(0)} = \lim_{\mathbf{q} \rightarrow 0} \lim_{\omega \rightarrow 0} \frac{(2\pi)^2}{\mathbf{q}^2} (\Pi_{11} + \Pi_{22}) \quad (\text{S31})$$

$$1/\kappa = \varpi^{(i)} = \lim_{\mathbf{q} \rightarrow 0} \frac{(2\pi)^2}{\mathbf{q}^2} \Pi_{00} = \lim_{\omega \rightarrow 0} \lim_{\mathbf{q} \rightarrow 0} \frac{(2\pi)^2}{\omega^2} \Pi_{ii} = \chi \quad (\text{S32})$$

where χ is, by definition, the polarizability of ψ . Note that the order of limits matters in the above expressions.

REVIEW ON DISORDERED ELECTRONS IN LANDAU LEVELS

In this section we review some known results for disordered electrons in Landau levels.

The density of states

The density of states within self-consistent Born approximation (SCBA) and under the assumption $\omega_c \tau \ll 1$ (τ is the scattering time and $\omega_c = B/m$ is the cyclotron frequency) reads as

$$D(\mathcal{E}) = \frac{m}{2\pi} \left(1 + 2 \sum_{k=1} (-1)^k e^{-\frac{\pi k}{\omega_c \tau}} \cos \left(\frac{2\pi k \mathcal{E}}{\omega_c} \right) \right) \quad (\text{S33})$$

Here k labels different harmonics. This expression is expected to work well in the strongly disordered limit $\omega_c \tau \ll 1$, and not too close to the bottom of the band. The lowest order approximation in $\mathcal{O}(\exp(-1/\omega_c \tau))$ is

$$D(\mathcal{E}) \approx \frac{m}{2\pi} \quad (\text{S34})$$

In the opposite limit $\omega_c \tau \gg 1$, we find

$$D(\mathcal{E}) = \sum_{n=0} \frac{B\Gamma_n(\mathcal{E})}{\pi^2 \Gamma}, \quad \Gamma_n(\mathcal{E}) = \text{Re} \sqrt{(\mathcal{E} - \omega_c(n + 1/2))^2 - \Gamma^2}, \quad \Gamma = \sqrt{\frac{2\omega_c}{\pi\tau}} \ll \omega_c \quad (\text{S35})$$

which is just a collection of semicircular broadened (but still non-overlapping) Landau levels. We note that the square root spectral edge is just an artifact of SCBA: in principle, there is always a Lifshitz tail leaking into the gap.

The position of the delocalized states

We follow the two-parameter scaling argument to obtain the critical density at which the delocalized states crosses the Fermi level. It was suggested that the conductivities should scale as [5–7]

$$\begin{aligned} \sigma_{xx}^{(0)} &= \frac{\sigma_0}{1 + (\omega_c \tau)^2} \\ \sigma_{xy}^{(0)} &= \frac{\sigma_0 \omega_c \tau}{1 + (\omega_c \tau)^2} \end{aligned} \quad (\text{S36})$$

where $\sigma_0 = \rho\tau/m$ is the bare Drude conductivity at $B = 0$. The condition for the n -th extended state being at the Fermi level is

$$\sigma_{xy}^{(0)} = \left(n + \frac{1}{2}\right) \frac{e^2}{h} \quad (\text{S37})$$

This means that the critical density needs to satisfy

$$\rho_c^{(n)} = \frac{B}{2\pi} \left(n + \frac{1}{2}\right) \frac{1 + (\omega_c\tau)^2}{(\omega_c\tau)^2} \quad (\text{S38})$$

In both the weak ($\omega_c\tau \gg 1$) and strong ($\omega_c\tau \ll 1$) limits, this expression reproduces asymptotically exact results; for intermediate regime, the result can be systematically improved using the self-consistent Born approximation, which we do not include in this work.

The Mott's law for conductivity

Here we review the derivation celebrated Mott's law on conductivity in Anderson insulators, which applies to the cases where the Fermi level is within the localized states. The goal is essentially to evaluate the current-current correlation:

$$\Pi^{ii}(\mathbf{q} = 0, \omega) = \langle J^i(\omega) J^i(-\omega) \rangle = \sum_{\epsilon_n < \mu, \epsilon_m > \mu} |\langle \psi_n | J^i | \psi_m \rangle|^2 \left[\frac{1}{\omega - \epsilon_{mn} + i0^+} - \frac{1}{\omega + \epsilon_{mn} + i0^+} \right] \quad (\text{S39})$$

where n, m are single particle eigenstate labels and μ is the chemical potential, and J is the total current operator. We will make the following assumptions to approximately evaluate this sum:

- Every state ψ_n is localized within a localization length $\xi_n \sim \xi(\epsilon_n)$, which is determined by the energy. The corresponding characteristic energy scale (typical level splitting) is $\delta_n \equiv 1/\mathcal{D}_0(\epsilon_n)\xi_n^d$ where \mathcal{D}_0 is the density of state and d is the spatial dimension.
- The overlap integral can be approximated as

$$|\langle \psi_n | J^i | \psi_m \rangle| \approx |\mathbf{R}_i| \bar{\delta} e^{-R/\bar{\xi}} \quad (\text{S40})$$

where $\bar{\delta} = \sqrt{\delta_n \delta_m}$, $\bar{\xi} = \frac{2\xi_n \xi_m}{\xi_n + \xi_m}$, and $R \sim |\mathbf{R}_i| \sqrt{d}$ is the separation between the centers of ψ_n and ψ_m .

- The sum can be approximated with a integral over the two energies and the separation between the two states

$$\sum_{\epsilon_n < \mu, \epsilon_m > \mu} \rightarrow \int_{\epsilon_1 < \mu} \int_{\epsilon_2 > \mu} \int_{\mathbf{R}} P(\epsilon_1, \epsilon_2, \mathbf{R}) \quad (\text{S41})$$

where P is the joint probability for given energies and the relative distance of the coordinates of two localized states.

- There is level repulsion if two localized states are too close, i.e.

$$P(\epsilon_1, \epsilon_2, \mathbf{R}) \approx \begin{cases} 0 & \epsilon_{21} < \bar{\delta} e^{-R/\bar{\xi}} \\ \mathcal{D}_0(\epsilon_1) \mathcal{D}_0(\epsilon_2) & \text{otherwise} \end{cases} \quad (\text{S42})$$

Putting everything together, we have the expression

$$\Pi^{ii}(\mathbf{q} = 0, \omega) \sim \int_{\epsilon_1 < \mu} \mathcal{D}_0(\epsilon_1) \int_{\epsilon_2 > \mu} \mathcal{D}_0(\epsilon_2) \int_{R^*}^{\infty} R^{d-1} dR \frac{\epsilon_{21} R^2 \bar{\delta}^2 e^{-2R/\bar{\xi}}}{(\omega + i\delta)^2 - \epsilon_{21}^2} \quad (\text{S43})$$

where $R^* = \max(\bar{\xi} \ln \frac{\bar{\delta}}{\epsilon_{21}}, 0)$. Evaluating the integral over R , we obtain

$$\Pi^{ii}(\mathbf{q} = 0, \omega) \sim \int_{\epsilon_1 < \mu} \mathcal{D}_0(\epsilon_1) \int_{\epsilon_2 > \mu} \mathcal{D}_0(\epsilon_2) \frac{\epsilon_{21} \bar{\xi}^{d+2} \bar{\delta}^2 \Gamma(d+2, 2R^*/\bar{\xi})}{(\omega + i0^+)^2 - \epsilon_{21}^2} \quad (\text{S44})$$

The imaginary part of this integral for small ω is straightforward to evaluate. Using $\frac{1}{x \pm i0^+} = P\frac{1}{x} \mp i\pi\delta(x)$, we obtain:

$$\text{Im}[\Pi^{00}(\omega)] \sim \mathcal{D}_0^2(\mu)|\omega|\xi^{d+2}(\mu)\bar{\delta}^2\Gamma(d+2, 2\ln\frac{\bar{\delta}}{|\omega|}) \sim i\mathcal{D}_0^2\omega^3\xi^{d+2}\left[\ln\frac{\bar{\delta}}{|\omega|}\right]^{d+1} \quad (\text{S45})$$

where all the quantities are evaluated at the Fermi energy. This reproduces the Mott's law

$$\text{Re}[\sigma(\omega)] = \text{Im}[\Pi^{00}(\omega)]/(i\omega) \sim \omega^2[\ln|\omega|]^3\xi^{d+2}\mathcal{D}_0^2 \quad (\text{S46})$$

The real part of the integral for small ω needs a bit more care, for which we use the identity

$$P\int_0^\infty \frac{f(x)}{x^2 - y^2}dx = \sum_{n=0}^\infty y^{2n}\int_0^\infty \frac{f(x)}{x^{2n+2}}dx \quad (\text{S47})$$

so that the small ω expansion to the leading nontrivial order is

$$\text{Re}[\Pi^{ii}(\omega)] \sim \omega^2 \int_{\epsilon_1 < \mu} \mathcal{D}_0(\epsilon_1) \int_{\epsilon_2 > \mu} \mathcal{D}_0(\epsilon_2) \bar{\xi}^{d+2} \bar{\delta}^2 \Gamma(d+2, 2R^*/\bar{\xi})/\epsilon_{21}^3 \quad (\text{S48})$$

The above integral is dominated by the contribution from the small $\epsilon_{21} \lesssim \bar{\delta}$ region where both $\epsilon_{1,2}$ are close to fermi level since $\Gamma(d+2, 2\ln\frac{\bar{\delta}}{\epsilon_{21}})/\epsilon_{21}^3 \sim \epsilon_{21}^{-1}[\ln\frac{\bar{\delta}}{\epsilon_{21}}]^{d+1}$ diverges for small ϵ_{21} . Therefore, we approximately have

$$\text{Re}[\Pi^{ii}(\omega)] \sim \mathcal{D}_0^2\omega^2\xi^{d+2}\bar{\delta} \quad (\text{S49})$$

where all the quantities are evaluated at the fermi energy. This implies a finite polarizability [3]

$$\text{Im}[\sigma(\omega)] = \text{Re}[\Pi^{00}(\omega)]/(i\omega) \sim \omega\xi^2\mathcal{D}_0 \implies \chi \sim \xi^2\mathcal{D}_0 \quad (\text{S50})$$

The polarizability in the weak disorder limit

In the weak disorder limit, the chemical potential still lies in the gap between LLs at integer fillings (neglecting the effects of exponentially small Lifshitz tail). The polarizability in this case with n filled LLs is evaluated [2] as

$$\chi = \frac{n}{4\pi\omega_c} \left(1 - \frac{\pi}{6\omega_c\tau}\right) \mathbf{q}^2 \quad (\text{S51})$$

EFFECTS OF PERPENDICULAR MAGNETIC FIELD

In this section we use the results of the previous sections to discuss the stability of the anyon superconductor, as well as the response of re-entrant IQH state, against applied magnetic field.

Anyon superconductor

Based on Eq. S3, we see that the effective magnetic field seen by the low-energy $\psi_{2/3}$ particles in the valleys is

$$\frac{B_{\text{eff}}}{2\pi} \equiv \frac{\nabla \times \mathbf{a}}{2\pi} + \frac{1}{3} \frac{1}{\mathcal{A}_{\text{UC}}} = \frac{2}{3} \frac{B}{2\pi} - \frac{1}{3} \rho_{2/3} \quad (\text{S52})$$

Therefore the effective cyclotron frequency

$$\omega_c = \frac{2\pi}{m_{2/3}} \left| \frac{1}{3} \rho_{2/3} - \frac{2}{3} \frac{B}{2\pi} \right| \quad (\text{S53})$$

where $m_{2/3}$ is the effective mass of $\psi_{2/3}$. On the other hand, the density is given by deviation the filling fraction of electrons from $\nu = 2/3$:

$$\rho_{2/3}\mathcal{A}_{\text{UC}} = \frac{3}{2}\delta\nu - \delta\nu_B \quad (\text{S54})$$

where $\delta\nu_B \equiv \frac{B\mathcal{A}_{\text{UC}}}{2\pi}$ is the external flux ‘filling fraction’ per unit cell. For convenience, we will parametrize

$$\omega_c\tau \equiv \tilde{\tau} |\delta\nu - 2\delta\nu_B| \quad (\text{S55})$$

where $\tilde{\tau} \equiv \frac{\pi\tau}{m_{2/3}\mathcal{A}_{\text{UC}}}$ is a dimensionless measure of the disorder strength.

We are now ready to discuss the stability of anyon superconductor in the presence of magnetic field. The transition point out of the superconducting regime, by our theory, is determined by when the 0-th (or 1-st) de-localized states in the three valleys simultaneously cross the Fermi level. Using Eq. S38, we find these two boundaries should be determined by setting $n = 0, 1$ in the below equation

$$\begin{aligned} -\frac{1}{3}\rho_{2/3} &= \frac{B_{\text{eff}}}{2\pi} \left(n + \frac{1}{2}\right) \frac{1 + (\omega_c\tau)^2}{(\omega_c\tau)^2} \\ \Rightarrow \tilde{\tau}^2 \left(\delta\nu - \frac{2}{3}\delta\nu_B\right) (\delta\nu - 2\delta\nu_B) &= \left(n + \frac{1}{2}\right) [1 + (\delta\nu - 2\delta\nu_B)^2 \tilde{\tau}^2] \end{aligned} \quad (\text{S56})$$

It should be noted that, in reality, the FQAH state spontaneously breaks the time reversal symmetry and we have implicitly assumed that the $B = 0$, $\nu = 2/3$ state has $2\pi\sigma_H = 2/3$. A *positive* B thus flips the Chern number of the parent state, and a time-reversed discussion should be applied in that case. Therefore, the current discussion is only relevant for $B < 0$.

Re-entrant integer quantum Hall state

The scenario of the RIQH state is more subtle since our theory suggests that the dispersion of $\psi_{1/3}$ may be quite shallow such that there is no LL degeneracy among the valleys. A crude approximation is to neglect the valleys caused by the discrete magnetic translation symmetry and apply the above analysis again, as we are doing below.

Based on Eq. S3, we see that the effective magnetic field seen by the low-energy $\psi_{1/3}$ particles is

$$\frac{B_{\text{eff}}}{2\pi} \equiv \frac{\nabla \times \mathbf{b}}{2\pi} + \frac{2}{3} \frac{1}{\mathcal{A}_{\text{UC}}} = \frac{1}{3} \frac{B}{2\pi} + \frac{2}{3} \rho_{1/3} \quad (\text{S57})$$

Therefore the effective cyclotron frequency

$$\omega_c = \frac{2\pi}{m_{1/3}} \left| \frac{2}{3} \rho_{1/3} + \frac{1}{3} \frac{B}{2\pi} \right| \quad (\text{S58})$$

where $m_{1/3}$ is the effective mass of $\psi_{1/3}$. On the other hand, the density is given by deviation the filling fraction of electrons from $\nu = 2/3$:

$$\rho_{1/3}\mathcal{A}_{\text{UC}} = 3\delta\nu - 2\delta\nu_B \quad (\text{S59})$$

Using a similar parametrization as the previous case,

$$\omega_c\tau = \tilde{\tau} |2\delta\nu - \delta\nu_B| \quad (\text{S60})$$

where $\tilde{\tau} \equiv \frac{2\pi\tau}{m_{1/3}\mathcal{A}_{\text{UC}}}$ is a dimensionless measure of the disorder strength.

The transition point out of the RIQH regime, by our theory, is determined by when the 0-th (or 1-st) de-localized state crosses the Fermi level. Using Eq. S38, we find these two boundaries should be determined by setting $n = 0, 1$ in the below equation

$$\tilde{\tau}^2 (3\delta\nu - 2\delta\nu_B) (2\delta\nu - \delta\nu_B) = \left(n + \frac{1}{2}\right) [1 + (2\delta\nu - \delta\nu_B)^2 \tilde{\tau}^2] \quad (\text{S61})$$

It should be noted that, in reality, the FQAH state spontaneously breaks the time reversal symmetry and we have implicitly assumed that the $B = 0$, $\nu = 2/3$ state has $2\pi\sigma_H = 2/3$. A *positive* B thus flips the Chern number of the parent state, and a time-reversed discussion should be applied in that case. Therefore, the current discussion is only relevant for $B < 0$.

In the main text, we plot these phase boundaries for a particular set of parameters: $\frac{2\pi\tau}{m\mathcal{A}_{UC}} = 20$ for $1/3$ anyons and $\frac{\pi\tau}{m\mathcal{A}_{UC}} = 40$ for $2/3$ anyons. Note that, $\tau_{1/3} = m_{1/3}n_{\text{imp}}(u/3)^2$ whereas $\tau_{2/3} = m_{2/3}n_{\text{imp}}(2u/3)^2$ by our assumptions. This means that $4m_{2/3} = m_{1/3}$ for the chosen parameters.

* These authors contributed equally to this work.

- [1] Alexander G. Abanov and Andrey Gromov. Electromagnetic and gravitational responses of two-dimensional noninteracting electrons in a background magnetic field. *Phys. Rev. B*, 90:014435, Jul 2014.
- [2] IS Burmistrov. Two-dimensional electron liquid with disorder in a weak magnetic field. *Journal of Experimental and Theoretical Physics*, 95:132–144, 2002.
- [3] M V Feigel'man, D A Ivanov, and E Cuevas. Dielectric response of anderson and pseudogapped insulators. *New Journal of Physics*, 20(5):053045, may 2018.
- [4] Andrey Gromov, Gil Young Cho, Yizhi You, Alexander G. Abanov, and Eduardo Fradkin. Framing anomaly in the effective theory of the fractional quantum hall effect. *Phys. Rev. Lett.*, 114:016805, Jan 2015.
- [5] D.E. Khmel'nitskii. Quantization of hall conductivity. *JETP Lett.*, 38 (9):552–556, 1983.
- [6] R. B. Laughlin. Levitation of extended-state bands in a strong magnetic field. *Phys. Rev. Lett.*, 52:2304–2304, Jun 1984.
- [7] R. B. Laughlin, Marvin L. Cohen, J. M. Kosterlitz, Herbert Levine, Stephen B. Libby, and Adrianus M. M. Pruisken. Scaling of conductivities in the fractional quantum hall effect. *Phys. Rev. B*, 32:1311–1314, Jul 1985.
- [8] Nathan Seiberg, T. Senthil, Chong Wang, and Edward Witten. A duality web in 2+1 dimensions and condensed matter physics. *Annals of Physics*, 374:395–433, 2016.
- [9] Zhengyan Darius Shi and T Senthil. Doping a fractional quantum anomalous hall insulator. *arXiv preprint arXiv:2409.20567*, 2024.